



**Environmental
Science**
Processes & Impacts

**Comparison of Modeled and Measured Indoor Air
Trichloroethene (TCE) Concentrations at a Vapor Intrusion
Site: Influence of Wind, Temperature, and Building
Characteristics**

Journal:	<i>Environmental Science: Processes & Impacts</i>
Manuscript ID	EM-ART-12-2019-000567.R1
Article Type:	Paper

SCHOLARONE™
Manuscripts

ENVIRONMENTAL IMPACT STATEMENT

This research demonstrates the combined importance of weather conditions, building characteristics, and contaminant fate and transport processes on vapor intrusion processes. Both modeled data and field measurements indicate that building air exchange rates (AERs) vary across seasons and may influence indoor air contaminant concentrations; however, when preferential pathways are present, variability in mass entry rates likely play an even more significant role by influencing contaminant indoor air concentration fluctuations at buildings impacted by vapor intrusion.

1
2
3 **Comparison of Modeled and Measured Indoor Air Trichloroethene**
4 **(TCE) Concentrations at a Vapor Intrusion Site: Influence of Wind,**
5
6 **Temperature, and Building Characteristics**
7
8
9

10
11
12 Elham Shirazi^a, Gregory S. Hawk^b, Chase W. Holton^c, Arnold J. Stromberg^b, Kelly G. Pennell*^a
13
14
15
16
17

18
19 ^a University of Kentucky, Department of Civil Engineering, Lexington, KY 40506, USA.
20
21

22
23 ^b University of Kentucky, Department of Statistics, Lexington, KY 40506, USA.
24
25

26 ^c Geosyntec Consultants, Inc., Denver, CO 80111, USA.
27
28

29 *Corresponding Author: email: kellypennell@uky.edu, Phone: +1 (859) 218-2540, Fax:
30
31

32 +1 (859) 257-4404
33
34
35

36 **ABSTRACT**
37
38

39
40 There is a lack of vapor intrusion (VI) models that reliably account for weather conditions
41 and building characteristics, especially at sites where active alternative pathways, such as sewer
42 connections and other preferential pathways, are present. Here, a method is presented to
43 incorporate freely-available models, CONTAM, and CFD0, to estimate site-specific building air
44 exchange rates (AERs) and indoor air contaminant concentrations by accounting for weather
45 conditions and building characteristics at a well-known VI site with a land drain preferential
46 pathway. To account for uncertainty in model input parameters that influence indoor air
47 chlorinated volatile organic compound (CVOC) concentration variability, this research
48
49
50
51
52
53
54
55
56
57

1
2
3 incorporated Monte Carlo simulations and compared model results with retrospective field data
4 collected over approximately 1.5 years from the study site. The results of this research show that
5 mass entry rates for TCE are likely influenced by indoor air pressures that can be modeled as a
6 function of weather conditions (over seasons) and building characteristics. In addition, the results
7 suggest that temporal variability in indoor air TCE concentrations is greatest (modeled and
8 measured) due to the existence of a land drain, which acts as a preferential pathway, from the
9 subsurface to the granular fill beneath the floor slab. The field data and modeling results are in
10 good agreement and provide a rare comparison of field data and modeling results for a VI site.
11 The modeling approach presented here offers a useful tool for decision makers and VI practitioners
12 as they assess these complex and variable processes that have not been incorporated within other
13 VI models.
14
15
16
17
18
19
20
21
22
23
24
25
26
27
28
29
30
31
32
33
34
35
36
37
38
39
40
41
42
43
44
45
46
47
48
49
50
51
52
53
54
55
56
57
58
59
60

INTRODUCTION

Hundreds of thousands of hazardous waste sites exist throughout many rural and urban communities in the United States. According to the National Research Council¹, some of the most persistent and pervasive legacy contaminants at hazardous waste sites include chlorinated volatile organic compounds (CVOC). A challenge for those tasked with managing CVOC exposure risks in communities near hazardous waste sites is vapor intrusion—the transport of vapors from subsurface sources into indoor spaces.

Characterizing the vapor intrusion (VI) pathway and related exposure risks at sites with CVOCs in soil and/or groundwater can be difficult because indoor air concentrations can vary temporally and spatially²⁻⁵. Some possible explanations for the observed variability in indoor concentrations are: (a) presence of alternative pathways for CVOCs to enter buildings at vapor intrusion sites^{3, 6-8}, and (b) a lack of understanding about how weather conditions and building characteristics influence VI exposure risk variability⁹⁻¹².

For many years, models have been used to assist decision makers in understanding exposure risks and to inform professional judgement^{13, 14}. In addition, several three-dimensional models^{9, 11, 15, 16} have been developed to inform the VI scientific community about fate and transport processes that govern exposure risks and drive risk management decisions.

Song et al.¹⁷ indicated that both contaminant soil gas entry rate and the building's ventilation rate depend on weather conditions. In another study, Song et al.¹⁸ investigated the influence of building tightness and climate variability on indoor air quality and showed energy efficient houses, in which indoor air is less likely to be replaced by outdoor air, can have higher vapor intrusion exposure risks. Luo⁹ modified the model developed by Abreu and Johnson¹⁵ to

1
2
3 evaluate the effect of wind flow on contaminant indoor air concentration; however, wind and
4 building characteristics effects on building AER was not directly assessed in this study.
5
6
7

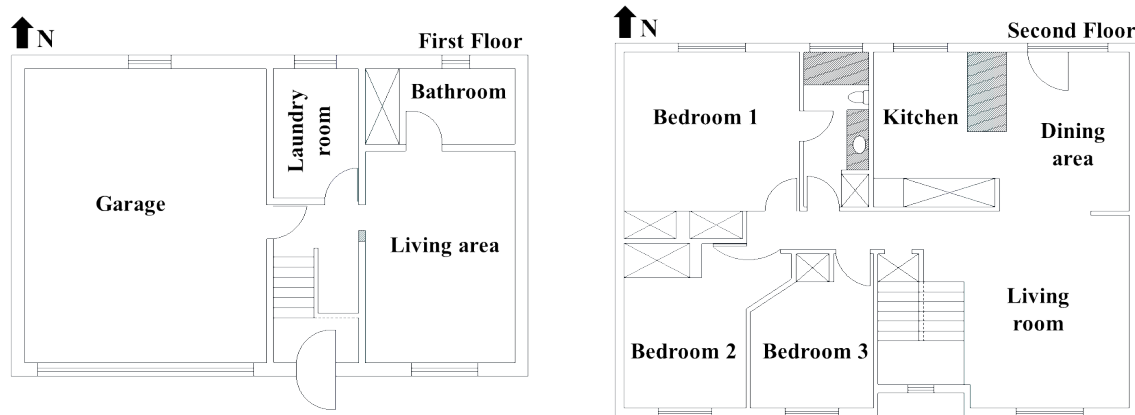
8 Recently, Shirazi and Pennell¹¹ developed a VI modeling approach in which building
9 science simulation tools were applied to evaluate the influence of weather and building conditions
10 on building AER and indoor air concentration. The results highlighted that similar and neighboring
11 buildings with the same weather conditions can have different indoor air quality because of
12 different indoor pressure and air exchange rates related to specific building characteristics.
13
14
15
16
17
18

19
20 In the present study, we apply the modeling approach suggested by Shirazi and Pennell¹¹
21 and Shirazi et al.¹⁹ to model a house in which indoor air CVOC concentrations and AERs were
22 measured over many months by Arizona State University^{2, 3, 20, 21}. The model considers weather
23 conditions, seasonal effects, and building characteristics to estimate building AERs and indoor air
24 concentrations. In addition, this study incorporates Monte Carlo simulations to consider high
25 uncertainty model input parameters.
26
27
28
29
30
31
32
33

34 35 **Site Description**

36
37 The site investigated in this study has been the focus of VI research since 2010^{2, 3, 20, 21}.
38 The building, referred to as the “study house” (photograph included in Supporting Information,
39 Figure S1), is located in Layton, Utah; and south of Hill Air Force Base Superfund site. The study
40 house is a two-story residential building with approximately 2.5 m elevation drop from back yard
41 to front yard. The building dimensions are 11.7 m × 8.7 m × 7.5 m which are length, width and
42 height of building, respectively. Figure 1 shows a schematic of study house floor plan. A
43 groundwater plume contaminated with 1,1-dichloroethene (1,1-DCE), 1,1,1-trichloroethane
44 (1,1,1-TCA) and trichloroethylene (TCE) is within the vicinity of the study house. Holton et al.²
45
46
47
48
49
50
51
52
53
54
55
56
57
58
59
60

1
2
3 reported 10-50 $\mu\text{g/L}$ average concentration of dissolved TCE in groundwater beneath the building.
4
5 TCE concentrations detected in indoor air were associated with subsurface TCE vapor sources^{2, 3}.
6
7



22 Figure 1: Schematic of study house floor plan showing first and second floor.

23 24 **Modeling Approach**

25
26 Figure 2 describes the modeling process, including required data input/output for the study
27 house. This research incorporates a multizone indoor air quality computer program (CONTAM)
28 coupled with computational fluid dynamics program (CFD0) which were developed by and are
29 freely available through the Building and Fire Research Laboratory of the National Institute of
30 Standards and Technology (NIST)²². These programs have been used previously by Shirazi and
31 Pennell¹¹ to investigate the influence of weather conditions and building characteristics on building
32 AER and indoor air concentration. Herein, CFD0 is coupled with CONTAM to investigate the
33 influence of weather conditions (wind and temperature) and building characteristics of the study
34 house to estimate building AER and indoor air concentration and compare results with measured
35 data in study house. CFD0 solves a turbulence model such as the Reynolds Averaged Navier-
36 Stokes equations to calculate the distribution of wind pressure on the building envelope. Wind
37 pressure is then converted to pressure coefficient (C_p) values using Bernoulli's equation. In
38 CONTAM, flow path locations are determined and CFD0 is linked to CONTAM to get the C_p
39
40
41
42
43
44
45
46
47
48
49
50
51
52
53
54
55
56
57
58
59
60

values relevant to each pathway. Afterwards, CONTAM calculates indoor air pressure by solving mass balance equations for all the indoor zones. Theoretical methodology of CONTAM and CFD0 and how these two models are connected is explained in Shirazi and Pennell¹¹. Shirazi and Pennell¹¹ determined mass entry rate of contaminant through the foundation cracks using a CFD modeling approach for VI and used it as the input in CONTAM to estimate indoor air concentration based on weather and building conditions (See Figure 1 in Shirazi and Pennell¹¹). Herein, the mass entry rate measured by Holton et al.²⁰ is used to develop probability distribution functions and to model mass entry rate of contaminant as a random variable for Monte Carlo simulations as an input in CONTAM, as discussed below.

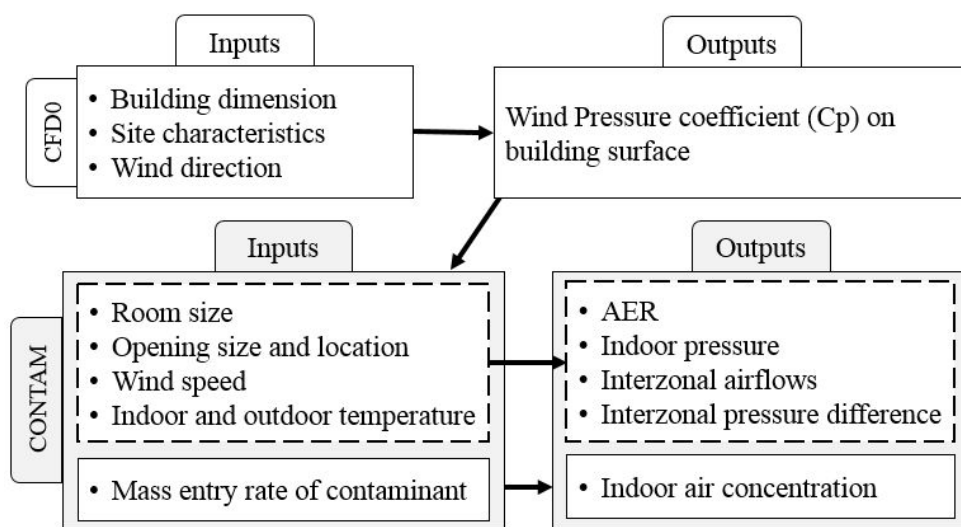


Figure 2: Modeling process by coupled CFD0 and CONTAM for the study house

Model input related to weather condition such as outdoor temperature, wind speed, and wind direction are collected from Ogden-Hinckley airport weather station and reported by previous studies.^{2, 20} Other inputs related to building characteristics such as rooms' size, openings' size and

1
2
3 location were collected by the authors. The list of inputs are shown in Table 1. Specific model
4
5 input values are provided in Supporting Information (Table S1-S3 and Figure S2).
6
7

8 Holton et al.² reports windows and doors were kept closed during sampling activities,
9
10 therefore windows and doors connected to outdoor areas are assumed to be closed in the model
11
12 and the only pathway through the building is the leakage through windows, doors and external
13
14 walls. Internal doors that connect different zones (rooms) to each other are observed and modeled
15
16 as open. Open exterior doors and windows, as well as other occupant behaviors, can influence
17
18 exposure risks;^{10, 23} and the modeling approach presented herein can account for these factors, as
19
20 necessary. Effective leakage area is an input in CONTAM that estimates the leakage area for closed
21
22 openings based on type and size of openings. The values of leakage areas used in this study are
23
24 provided in Supporting Information Table S3.
25
26
27
28
29
30
31
32
33
34
35
36
37
38
39
40
41
42
43
44
45
46
47
48
49
50
51
52
53
54
55
56
57
58
59
60

Table 1: List of inputs related to study house used in CONTAM

Input	Range	Modeled values	Determined by
Outdoor temperature	-17 to 38 °C	-13, 7, 22 and 37°C	Holton et al. ²⁰ and based on ASHRAE Handbook of Fundamentals ²⁴
Indoor temperature	NR*	22°C	Measured by authors and based on ASHRAE Handbook of Fundamentals ²⁴
Wind speed	0-10 m/s	0, 1, 5 and 10 m/s	Holton et al. ^{2, 20}
Wind direction	0-360°	0, 15, 30, ..., 360°	NR*
Floor height	NR*	2.5 m	Measured by authors
Building dimension	NR*	11.7m× 8.7m×7.5 m	Measured by authors
Room size	NR*	See Table S1 and Figure S2 in supporting information	Measured by authors
Openings' relative elevation	NR*	See Table S2 and Figure S2 in supporting information	Measured by authors
Openings' effective leakage area (ELA)	Varies based on opening type	See Table S3	Suggested by ASHRAE Handbook of Fundamentals ²⁵

*NR- Not relevant.

We coupled CFD0 and CONTAM to consider both weather conditions and building characteristics effect on AER and indoor air concentration. Inputs in CFD0 (Figure 2) are related to overall building dimension such as width, length, total height of building including building's roof (2m height of roof with 20° slope); and local terrain features. Soils that surround part of building's walls from backyard to front yard are modeled which allows CFD0 to predict pressure coefficients (Cp) on building envelope properly.

1
2
3 In CFD0, atmospheric boundary layer thickness (δ_{met}) and the exponent at meteorological
4 station (α_{met}) are equal to 270m and 0.14, respectively which is in accordance with category of
5 open terrain with scattered obstructions (see Table 1, Chapter 24 of ASHRAE²⁴). The study house
6 is located in a residential neighborhood with two-story detached buildings. Considering the study
7 house site, it is assumed that the category terrain is an urban and suburban area with numerous
8 closely spaced obstructions. Therefore the δ and α values are equal to 370 m and 0.22, respectively
9 (More description related to δ and α values in Shirazi and Pennell¹¹). Herein, CFD0 simulates
10 different wind directions all around the building from 0° to 360° with 15° increments, considering
11 relative north to be zero wind direction for the study house.
12
13
14
15
16
17
18
19
20
21
22
23

24 Figure S3 in Supporting Information shows the air pressure profile around the study house
25 modeled using CFD0. Pressure on the building envelop is then converted to pressure coefficient
26 (Cp) relevant to each opening in CONTAM. As an example, Figure S4 in Supporting Information
27 indicates the pressure coefficient (Cp) calculated by CFD0 for opening number 11 in second floor
28 in CONTAM (Figure S2 and S4).
29
30
31
32
33
34
35
36
37
38

39 **Monte Carlo Simulations**

40

41
42 To account for uncertainty of model input parameters, the modeling approach uses Monte
43 Carlo simulations. Probability distribution functions account for uncertainty in input parameters
44 and these inputs are assigned as random variables. Three different scenarios are considered based
45 on different seasons including winter (December 21 to March 20), summer (June 21 to September
46 20) and shoulder (fall (September 21 to December 20) and spring (March 21 to June 20)) seasons.
47 In each scenario, four different inputs, including 1) outdoor temperature, 2) wind speed, 3) wind
48
49
50
51
52
53
54
55
56
57
58
59
60

1
2
3 direction; and 4) mass entry rate of contaminant, are modeled as random variables for Monte Carlo
4
5 simulations.
6
7

8 Retrospective field data collected at the study house was compared to the Monte Carlo
9
10 results. The study house provides a rare source of data. The availability of data in terms of frequency,
11
12 duration, and parameters is truly unique. The purpose of this research is to use retrospective data
13
14 that were collected under “natural vapor intrusion conditions” over multiple seasons. In general,
15
16 the study house has been described as having two conditions: 1) “natural condition” in which the
17
18 contaminant entered the study house by vapor intrusion driving forces via wind and stack effects;
19
20 2) Controlled-Pressure Method (CPM) condition in which building was under-pressurized by
21
22 blower fans for specific experimental purposes³, separate from this research. This research
23
24 incorporates data collected during condition 1 and focuses on multiple seasons to investigate
25
26 weather conditions, which constrained this retrospective analysis to data where the preferential
27
28 pathway at the study house was open.
29
30
31
32
33

34 Probability distribution functions are assigned based on the histograms and the range of
35
36 collected data (Table 2) and are used to generate random variables for wind direction using an up-
37
38 weighted uniform distribution; and random variables for outdoor temperature, wind speed and
39
40 mass entry rate are generated using truncated normal distributions. The probability distribution
41
42 functions used in Monte Carlo simulation are the functions that best match the data and histograms
43
44 of measured data. Truncated distributions can be utilized to restrict the domain of probability.
45
46 Considering the histograms of measured data for outdoor temperature, wind speed and mass entry
47
48 rate, truncated normal distribution are assigned to outdoor temperature and truncated lognormal
49
50 distribution is assigned to wind speed and mass entry rate to generate random variables.
51
52
53
54
55
56
57
58
59
60

1
2
3 An up-weighted uniform distribution is used for wind directions with a range of 0 to 360°
4 with 15° increments around the building (Figure 4 and Table 2). Holton et al.² reported that the
5 dominant wind direction for the study house was southern. Considering southern wind direction
6 to be 135° to 225° wind direction, random variables for wind direction are generated by an up-
7 weighted uniform distribution in which southern wind directions have double the chance of
8 happening.
9

10
11
12 Weather related inputs, such as wind speed and outdoor temperature for each season, were
13 obtained from Ogden-Hinckley airport weather station²⁶ for corresponding sampling days (days in
14 which AER and TCE indoor concentration were measured in study house under natural
15 conditions). Mean, minimum, maximum and standard deviation values (Table 2) obtained from
16 weather station are utilized to define the parameters of a truncated normal and truncated lognormal
17 distribution for outdoor temperature and wind speed, respectively.
18
19

20
21
22 TCE mass entry rate measured in the study house under “natural conditions” is used as
23 variable input. The TCE mass entry rate shows temporal variation based on different seasons, with
24 the greatest values in the winter and lowest in the summer (Figure 3). This variation is likely
25 influenced by the “preferential pathway”, which includes a land drain built to drain the foundation
26 of the study house and is connected to the storm sewer⁶. It was previously determined that this
27 land drain served as a preferential pathway for TCE to enter the building^{3, 6}. Mean, minimum,
28 maximum and standard deviation values for mass entry rate of contaminant (Table 2) are obtained
29 from the data collected by Holton et al.²⁰ under natural condition. These values are used to calculate
30 the parameters of a truncated lognormal distribution for mass entry rate of contaminant for Monte
31 Carlo simulations.
32
33
34
35
36
37
38
39
40
41
42
43
44
45
46
47
48
49
50
51
52
53
54
55
56
57
58
59
60

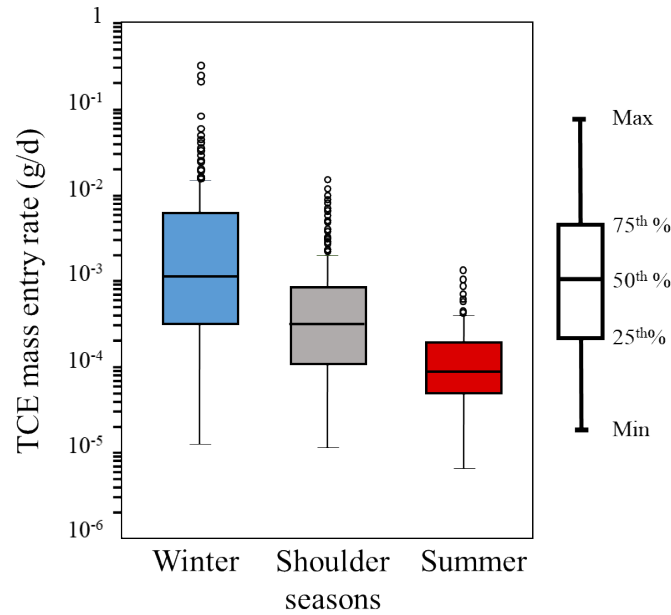


Figure 3: Temporal variations in TCE mass entry rate

Table 2 provides the random variables used in Monte Carlo simulation. Histograms of random draws for four random variables (outdoor temperature, wind speed, wind direction and mass entry rate of contaminant) used in Monte Carlo simulation in this study are shown in Figure S5 in supporting information.

To perform Monte Carlo simulations, the workflow was automated through integration of Monte Carlo's random variables and CONTAM (version 3.2) using an in-house script written in Python 3.6 by the authors. To automate CONTAM, authors modified CONTAM.PRJ file with assistance of CONTAM developers at NIST²². The Python 3.6 script was used to provide CONTAMX with Monte Carlo's random variables through command line and to collect CONTAMX's outputs upon simulation complement.

Table 2: Input parameters for Monte Carlo simulation

Seasons	Input parameter	Mean	Standard deviation	Min	Max	Type of distribution used in Monte Carlo simulation
Winter (21 December to March 20)	Outdoor temperature (°C)	0.79	6.2	-17	19	Truncated normal distribution
	Wind Speed (m/s)	5	4.8	0	23.7	Truncated lognormal distribution
	Wind direction (degree)	-	-	0	360	Up-weighted uniform distribution
	Mass entry rate of contaminant (g/d)	7.87×10^{-3}	2.78×10^{-2}	1.26×10^{-5}	3.20×10^{-1}	Truncated lognormal distribution
Shoulder seasons: Spring (March 21 to June 20) and Fall (September 21 to December 20)	Outdoor temperature (°C)	10.35	8.7	-11	36	Truncated normal distribution
	Wind Speed (m/s)	5.5	5.1	0	26.8	Truncated lognormal distribution
	Wind direction (degree)	-	-	0	360	Up-weighted uniform distribution
	Mass entry rate of contaminant (g/d)	1.11×10^{-3}	2.15×10^{-3}	1.15×10^{-5}	1.51×10^{-2}	Truncated lognormal distribution
Summer (June 21 to September 20)	Outdoor temperature (°C)	24.79	6.6	10	38	Truncated normal distribution
	Wind Speed (m/s)	5.7	5.1	0	24.6	Truncated lognormal distribution
	Wind direction (degree)	-	-	0	360	Up-weighted uniform distribution
	Mass entry rate of contaminant (g/d)	1.74×10^{-4}	2.20×10^{-4}	6.52×10^{-6}	1.32×10^{-3}	Truncated lognormal distribution

Note: Daily mean, minimum and maximum values for outdoor temperature and wind speed were adopted from Ogden-Hinckley airport weather station for duration of sample collection under natural condition. Mean, maximum, and minimum values for mass entry rate were obtained from mass entry rate values measured at the study house. Standard deviation for outdoor temperature, wind speed and mass entry rate of contaminant is calculated based on data collected at Ogden-Hinckley airport weather station and study house. For outdoor temperature, wind speed and mass entry rate of contaminant, the values for min, max, mean, and standard deviation were used to define the parameters of a truncated normal/lognormal distribution. Since dominant wind direction was reported to be southern wind direction, an up-weighted uniform distribution is considered for wind direction to address the higher chance of dominant wind direction.

RESULTS AND DISCUSSION

Study house AER: Weather condition and Building Characteristic Effects

To demonstrate the influence of weather conditions and building characteristics, the whole-house AER was estimated using the list of inputs in Table 1 (without random variables in Table 2). Figure 4 shows the variability in the modeled AER values, with the greatest values occurring when wind is the southern direction (135° - 225°). The purpose of this figure is to show the contextual understanding of AER and weather/building characteristics in the study house. The leaky side of the building is to the south, where the garage door is located. Based on previous research at the study house, the southern direction is the dominant wind direction² with most leakage areas. The lowest AERs (for each wind speed) occur when the wind blows on the tight sides of the building (90° and 270°). Figure 4 also indicates that for each specific wind speed and most wind directions, winter results in higher AER values, which is due to higher temperature differentials (indoor compared to outdoor) and summer results in lower AER due to lower temperature differentials.

Straight lines in Figure 4 indicate the outdoor air temperature effect with no wind flow (stack effect only) on AER. The blue straight line represents winter with largest AER value compared to other seasons which is due to higher temperature difference between indoors and outdoors. Other straight lines represent summer (37°C outdoor temperature) and shoulder season (with 7°C outdoor temperature) under stack effect only condition. These two straight lines are almost identical because of the same absolute temperature differential between indoor and outdoor (Shoulder: $|7-22|=15^{\circ}\text{C}$ and $|37-22|=15^{\circ}\text{C}$). The lowest AER estimated by the model ($<0.5\text{ d}^{-1}$) corresponds to a weather condition with no temperature difference between indoor and outdoor (shoulder season with 22°C outdoor temperature with wind speed less than or equal to 1 m/s),

which is a rare, nearly impossible, condition to sustain for any length of time. Because these conditions are unlikely to be observed in field settings, the scenario is not plotted in Figure 4 for simplification purposes.

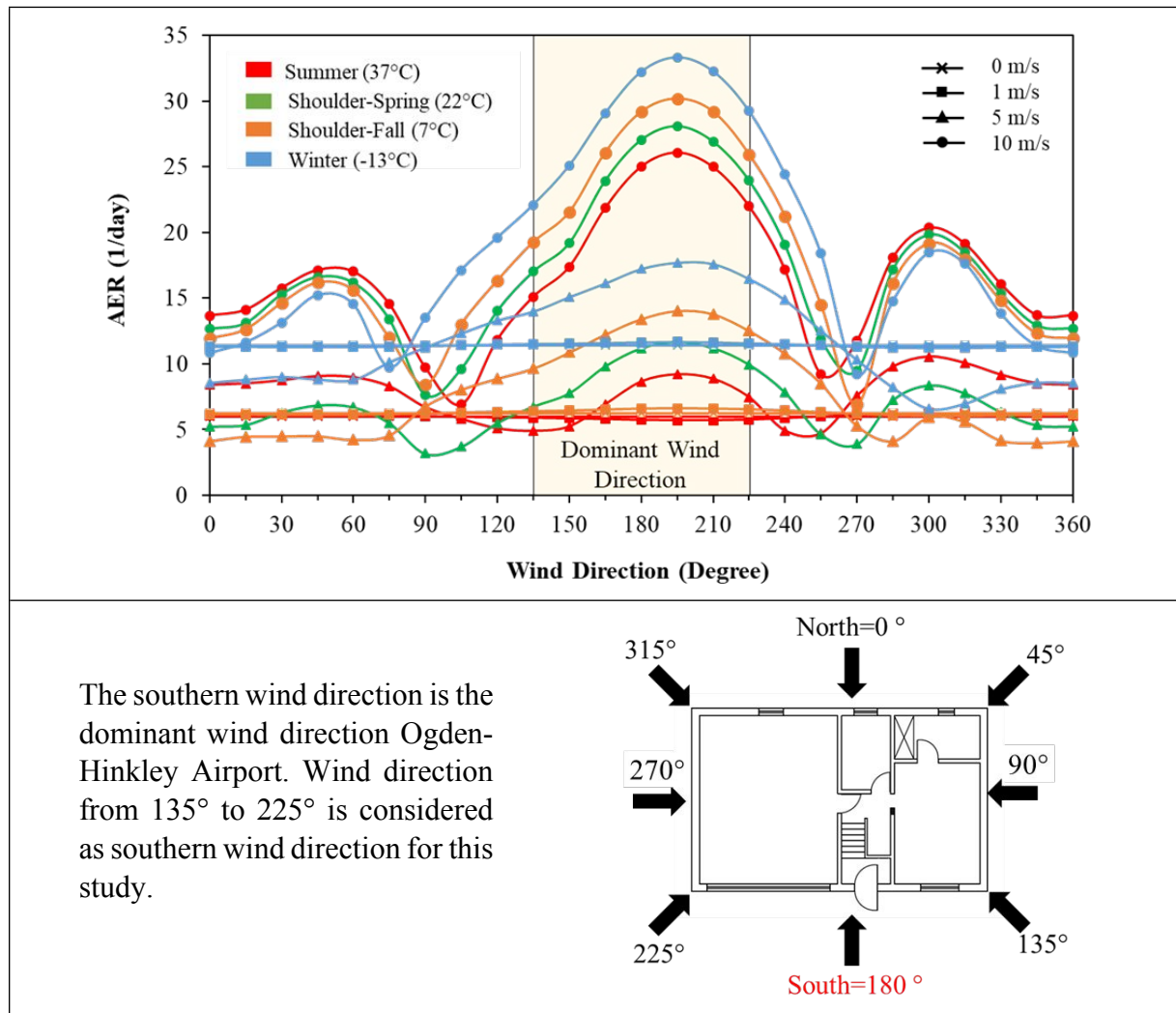


Figure 4: Modeled air exchange rates under different wind speeds, wind directions and outdoor air temperatures

AERs relevant to summer and shoulder seasons (e.g. fall and spring) are lower than the AERs calculated for winter due to lower temperature difference between indoor and outdoor in summer and shoulder seasons. Wind direction and building characteristics (such as opening location and or being leaky or tight) are important factors that control building's AER. Figure 4 shows that when 5 or 10 m/s wind blows on tight side of building (90° and 270°) AER drops to

1
2
3 values even lower than the values calculated for no wind flow scenario (stack effect). These
4 observations indicate that wind direction and building openings can impact the AER. The
5 importance of wind direction and building characteristics highlights the fact that similar buildings
6 at the same neighborhood can have different building AER and indoor air quality.
7
8
9
10
11
12

13 **Monte Carlo Simulation Results vs. Measured Values**

14 *AER Values:*

15
16
17
18
19 Because of uncertainty in weather conditions and mass entry rates, Monte Carlo
20 simulations were incorporated into this study to compare model results with measured values. AER
21 field measurements were conducted by others² using SF₆ (sulfur hexafluoride) tracer gas method
22 in the lower level of the study house. Figure 5a indicates measured AER values for winter, shoulder
23 and summer seasons. As shown in Figure 5a, winter and shoulder seasons indicate larger AER
24 values compared to summer. Model results estimate “whole-house” AER values (Figure 5b) and
25 indicate a wider range of AER for winter and summer compared to corresponding measured
26 values.
27
28
29
30
31
32
33
34
35
36

37
38 The model estimated and measured values are different for several possible reasons
39 including: 1) weather data used to generate random variables were from Ogden-Hinckley weather
40 station which was the nearest weather station to Layton, UT, while the weather condition at the
41 study site may have been different; 2) effective leakage area values considered in this study are
42 based on suggested values in ASHRAE Handbook of Fundamentals because site specific
43 measurements are not available 3) correlation between weather related inputs such as wind speed
44 and outdoor temperature were not addressed in this retrospective analysis because detailed data
45 related to occupant behavior (windows/doors open-closed and HVAC operation) and on-site
46 weather condition measurements were not available.
47
48
49
50
51
52
53
54
55
56
57

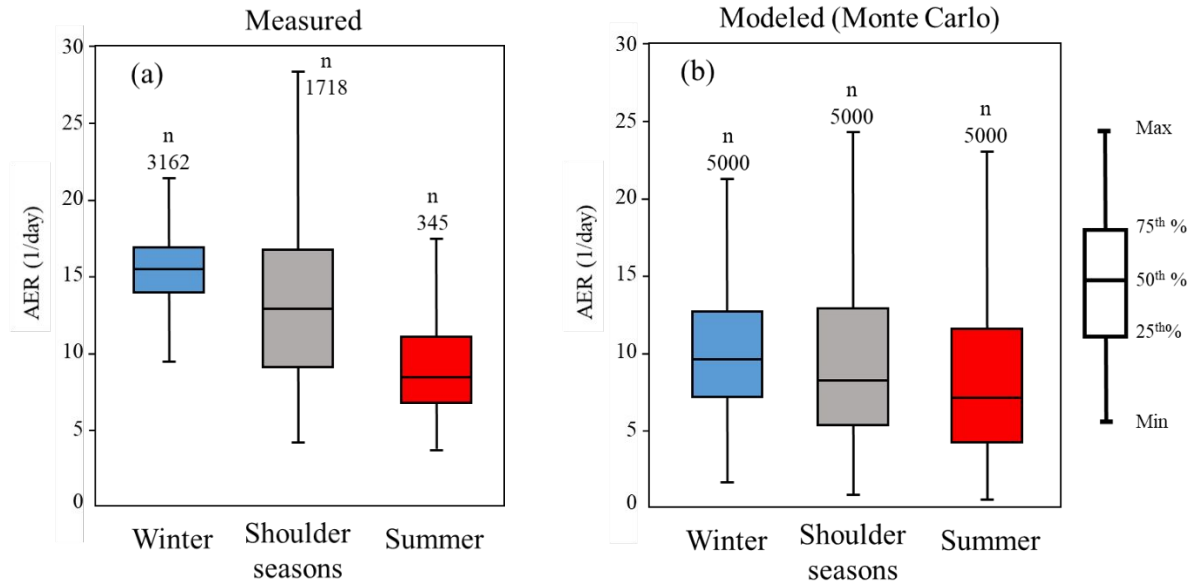


Figure 5: Box and whiskers plot of (a) Measured AER and (b) Modeled (Monte Carlo simulation) AER

Study house TCE indoor air concentration:

Figure 6 shows the measured indoor air TCE concentrations (Figure 6a) compared with modeled indoor air TCE concentrations (Figure 6b). The dashed horizontal line shown in Figure 6a at 0.008 ppbv is the detection limit for TCE concentration². The model predictions that are lower than the measured detection limits are not illustrated for comparison between measured data and model results (Figure 6b).

Comparing Figure 6a and 6b, the greatest indoor air TCE concentrations and variations corresponded to the winter season in model estimated concentrations, as well as field measured values. The lowest indoor air TCE concentrations and variations (modeled and measured) were detected in the summer. Additionally, the model estimated TCE concentrations follow the same seasonal variability as the field measurements. The greatest TCE concentration is predicted for winter, then shoulder seasons, with the lowest TCE concentration for the summer season. This trend is similar to the TCE mass entry rate temporal variation shown in Figure 3. Indicating that

TCE indoor air concentration is influenced by the TCE mass entry rate. For this study house the mass entry rate was greatly influenced by the presence of a land drain preferential pathway, which caused a large variation in TCE mass entry rates³. Strom et al.²⁷ statistically analyzed field data measured at the study house and noted similar observations between mass entry rate, indoor air concentrations and the presence of the preferential pathway.

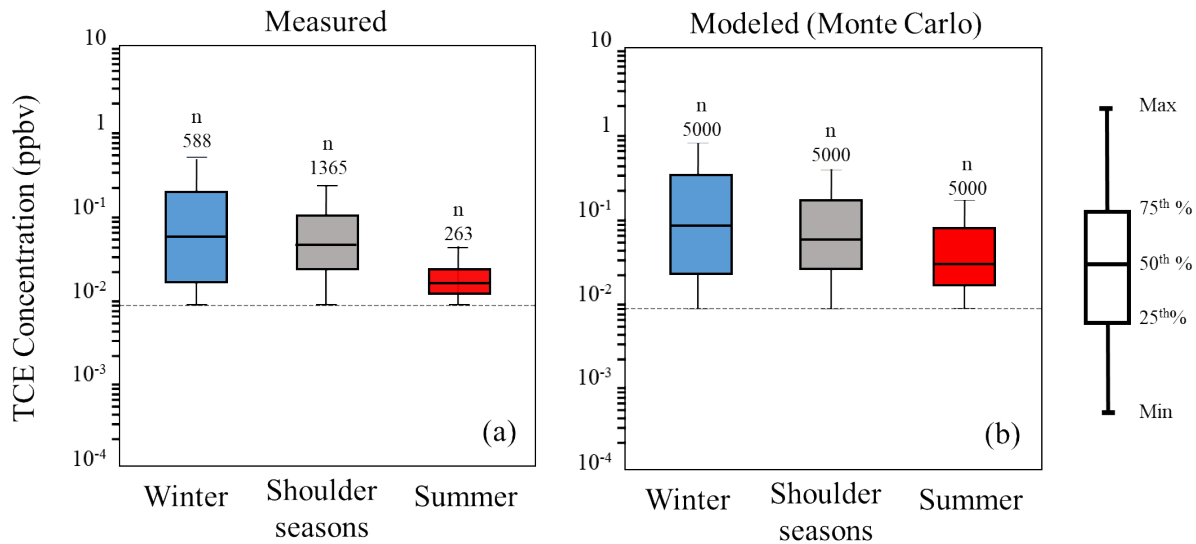


Figure 6: Box and whiskers plot of (a) Measured TCE concentration; (b) Modeled (Monte Carlo simulation) TCE Concentration excluding predicted values lower than detection limit

Note 1: The dashed horizontal line shown in Figures 6a, 6b at 0.008 ppbv is the detection limit for TCE concentration.²

Indoor pressure variations

Seasonal variability of indoor pressure can influence temporal variability of TCE mass entry rate which can consequently influence TCE indoor air concentrations. Although the driving force for mass entry rate is actually the pressure differential (i.e. the difference between indoor and outdoor pressure), Shirazi and Pennell¹¹ discuss that typically mass entry rate is conversely related to indoor pressure. The pressure on the building envelope varies at different points of a building. Therefore, there is not a specific indoor-outdoor pressure differential when wind speed is larger than zero, which negates the idea of a single pressure differential in conventional vapor intrusion studies.

Figure 7 compares the measured pressure differential for different seasons with the calculated indoor pressure. Although Figure 7a and 7b show two different parameters, they both follow the same trend. Figure 7a shows the 24-hour pressure differential between indoor and outdoor during sampling time. The indoor differential pressure reference location was co-located with the indoor air sampling location² and the outdoor differential pressure reference location was on the southeast corner of the house and underneath a slight overhang (Figure S6). Figure 7b shows the indoor pressure calculated by model in lower level of the study house (zones 1 and 2 in Figure S6) wherein TCE samples were collected. The study house is more under pressurized in winter than in shoulder seasons and summer, respectively. Figure 7 suggests that higher mass entry rates (Figure 3) may occur in the winter compared to summer and shoulder seasons because of lower indoor pressure.

CONTAM coupled with CFD0 calculates the indoor pressure in each level and zone of a building by solving a mass balance equation (See section Modeling Approach, and Shirazi and Pennell¹¹). Both calculated indoor pressure (in this study) and measured pressure differential (in

Holton et al.²⁾ are a function of wind speed, wind direction and temperature difference between indoors/outdoors and vary seasonally. Indoor pressures from the model ranged from -8.5 to +5.1 Pa in the study house (Figure 7b) and measured pressure differential ranged from -3.2 to +4.8 Pa (Figure 7a). These results suggest by considering calculated variation in indoor pressure of lower level of study house, decision makers can have a better judgment of mass entry rate and indoor air concentration variability.

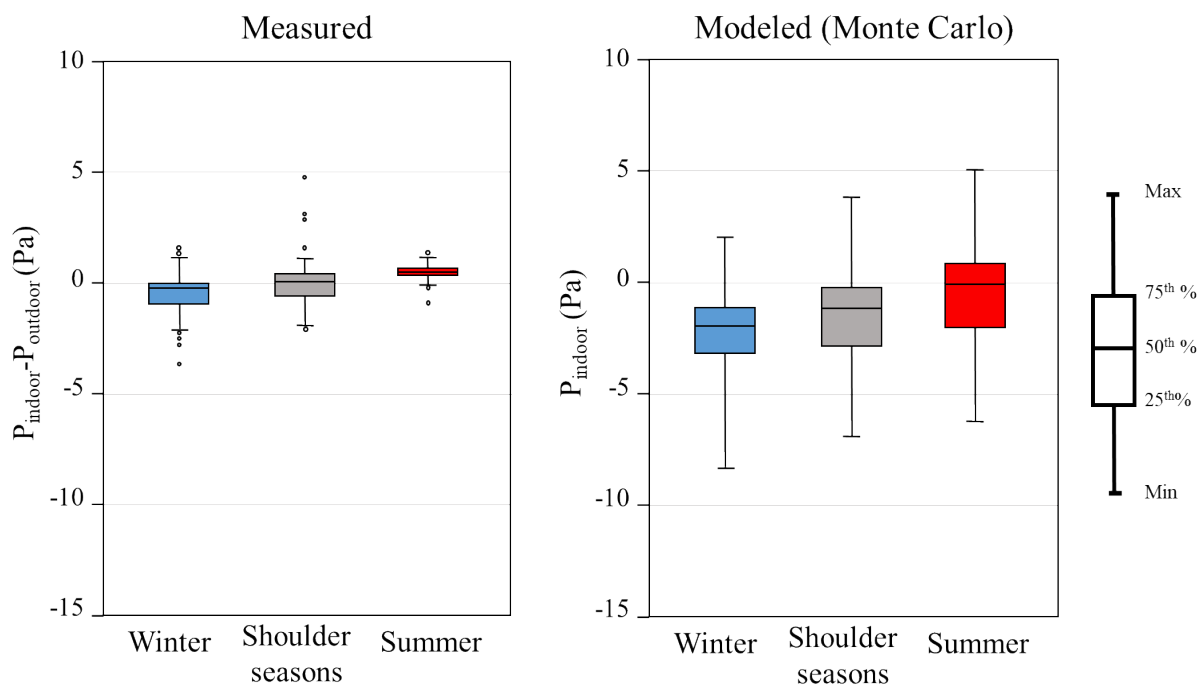


Figure 7: Box and whiskers plot of (a) Measured 24-hr pressure differential between indoor and outdoor and (b) Modeled (Monte Carlo simulation) indoor pressure variation caused by different weather conditions in study house

CONCLUSIONS

The research presented here is the first to demonstrate using both modeled data and field measurements how weather conditions, building characteristics, and contaminant fate and transport processes can be used to inform VI site assessments. To date, few, if any, VI models have attempted to compare indoor air concentration measurements with modeled indoor air concentration

1
2
3 estimates (see Figure 6). The data shown in Figure 6 is in good agreement, especially given the
4
5 uncertainty in the input parameters.
6
7

8 This research shows that variability in AER can be an important driver for indoor air
9
10 contaminant concentration variability (temporally and spatially) (Figures 4 and 5); however, when
11
12 preferential pathways are present, they may cause higher variability in indoor air concentrations due
13
14 to large variations (over 4-orders in magnitude) in mass entry rates (Figure 3). There are other factors
15
16 that have been investigated at this study house related to mass entry rate variability (e.g. Guo et al.
17
18 ³, and Holton et al.²⁰ and Guo ²⁸). One factor that has the potential to influence variations in mass
19
20 entry rates relates to the connection of the study house to the land drain preferential pathway³.
21
22 Preferential pathways that serve as a source for vapor intrusion exposure risks may experience
23
24 large contaminant concentration and flux variations within the pathways themselves, as reported
25
26 by Roghani et al.⁸ and Guo et al. ²⁹.
27
28
29

30 31 *Implications for Decision Makers* 32 33

34 To predict indoor air concentration, the modeling approach used in this research requires
35
36 the mass entry rate of contaminant to be input into the model (see Figure 2). Mass entry rate can
37
38 be obtained by several methods³⁰⁻³². Shirazi and Pennell¹¹ used a finite element model, which
39
40 considered weather conditions and building characteristics in the mass entry rate calculation, but
41
42 their approach is computationally expensive and likely too complicated to be widely used routinely
43
44 at vapor intrusion sites. They indicated that mass entry rate of contaminant is linearly related to
45
46 building indoor pressure. Another method that is more accessible to practitioners is the 2004 EPA
47
48 version of the Johnson and Ettinger (J&E) model^{33, 34}. The J&E model does not account for the
49
50 effect of weather conditions when estimating indoor air concentration, and, consequently, mass
51
52 entry rate of contaminant. For this research, when the alternative pathway was not active, the J&E
53
54
55
56
57
58
59
60

1
2
3 model appeared to approximate the mass entry. However, when the alternative pathway is active,
4
5 considerable temporal variability in mass entry rates occurred; and, higher mass entry rates were
6
7 required for the model to agree with the measurements³.
8
9

10 “Measured” mass entry rates can be obtained indirectly using indoor air contaminant
11
12 concentrations and air exchange rates. These values were used herein. We input mass entry rates
13
14 into the model that ranged from 0.32 g/d and 6.52x10⁻⁶ g/d (Table 2), which represent the range of
15
16 mass entry rates measured at the study house²⁰. The highest mass entry rates under natural
17
18 conditions for the study house occurred during the winter²⁰ (Figure 3). The lowest and least
19
20 temporally variable mass entry rates were observed when the alternative pathway was closed²⁰.
21
22 The mass entry rate reported for this period is comparable to the mass entry rate predicted by the
23
24 2004 EPA J&E spreadsheet.
25
26
27
28

29 For VI sites where temporal variability in indoor air concentrations has been observed and
30
31 a range of indoor air concentrations have been recorded, a similar approach could be used.
32
33 Decision makers who use Petroleum Vapor Intrusion Screening Model incorporates uncertain
34
35 analysis using Monte Carlo analysis³⁵. However, it should be noted that the field measurement
36
37 data used herein was high-resolution and availability of this type of data would be rare for a typical
38
39 site. Nonetheless, practitioners are challenged every day to make decisions in real-world settings
40
41 with limited data. Incorporating the models used in this research along with the typical data
42
43 available for a site could provide new insight for understanding exposure risks.
44
45
46
47

48 Mass entry rate (range), can be obtained from indoor air VOC concentration measurements
49
50 within a building.
51
52

$$M_{ER} = C_{indoor\ air\ (measured)} \times AER_{(CONTAM)} \times V_B \quad \text{Eq. 1}$$

53
54
55
56
57

1
2
3 Where,

4
5
6 M_{ER} is the mass entry rate of contaminant (g/d), $C_{\text{indoor air (measured)}}$ is the indoor air
7 concentration of contaminant that has been measured during different sampling events (g/m³),
8
9
10 $AER_{(CONTAM)}$ is the range of AER calculated by CONTAM considering weather condition and
11 building characteristics (d⁻¹) and V_B is the volume of building. As shown on Figure 2, AER can be
12 calculated by CONTAM independently of the indoor air concentration. Figure 4 demonstrates,
13 using the study house as an example, that AER is a function of wind direction, wind speed and
14 building characteristics. Practitioners could determine a range of mass entry rates and model
15 variability in indoor air concentrations using CONTAM and obtain output similar to that shown in
16 Figure 6.
17
18
19
20
21
22
23
24
25

26
27 At sites where obtaining mass entry rates using existing indoor air VOC concentrations is
28 not possible, the 2004 EPA spreadsheet version of the J&E model^{31, 32} is another option for
29 estimating mass entry rates, but this approach would assume that an alternative pathway does not
30 exist. Mass entry rate of contaminant can be calculated using Equation 2.
31
32
33
34
35

$$36 \quad M_{ER} = C_{J\&E} \times AER_{(CONTAM)} \times V_B \quad \text{Eq. 2}$$

37
38
39 Where,

40
41
42 M_{ER} is the mass entry rate of contaminant (g/d), $C_{J\&E}$ is the indoor air concentration of
43 contaminant calculated by EPA spreadsheet when there is no alternative pathway (g/m³),
44
45
46
47 $AER_{(CONTAM)}$ is the range of AER calculated by CONTAM considering weather condition and
48 building characteristics (d⁻¹) and V_B is the volume of building.
49
50
51
52
53
54
55
56
57
58
59
60

1
2
3 Once mass entry rates are obtained, the approach used for modeling the study house in this
4
5 research would allow practitioners to cost-effectively evaluate variability in exposure risks (e.g.
6
7 indoor air concentrations) based on weather conditions and building characteristics.
8
9

10 **CONFLICTS OF INTEREST:** The authors have declared no conflict of interest.
11
12

13
14 **ACKNOWLEDGMENTS:** The authors are grateful for the technical assistance of Dr. Paul
15
16 Dahlen at Arizona State University for access to and background information related to the study
17
18 house in Layton, UT. The authors deeply thank William Stuart Dols at the National Institute of
19
20 Standards and Technology (NIST) for assistance in automating CONTAM for Monte Carlo
21
22 simulations.
23
24
25

26
27 The project described was supported by University of Kentucky Superfund Research
28
29 Program from the National Institute of Environmental Health Sciences [Grant Number
30
31 P42ES007380] and by the National Science Foundation [Grant Number 1452800]. The content is
32
33 solely the responsibility of the authors and does not necessarily represent the official views of the
34
35 National Institute of Environmental Health Sciences, the National Institutes of Health or the
36
37 National Science Foundation.
38
39
40
41
42
43
44
45
46
47
48
49
50
51
52
53
54
55
56
57
58
59
60

REFERENCES

1. National Research Council, Alternatives for Managing the Nation's Complex Contaminated Groundwater Sites. **2013**.
2. Holton, C.; Luo, H.; Dahlen, P.; Gorder, K.; Dettenmaier, E.; Johnson, P. C., Temporal Variability of Indoor Air Concentrations under Natural Conditions in a House Overlying a Dilute Chlorinated Solvent Groundwater Plume. *Environmental Science & Technology* **2013**, *47*, (23), 13347-13354.
3. Guo, Y.; Holton, C.; Luo, H.; Dahlen, P.; Gorder, K.; Dettenmaier, E.; Johnson, P. C., Identification of Alternative Vapor Intrusion Pathways Using Controlled Pressure Testing, Soil Gas Monitoring, and Screening Model Calculations. *Environ Sci Technol* **2015**, *49*, (22), 13472-82.
4. Folkes, D.; Wertz, W.; Kurtz, J.; Kuehster, T., Observed Spatial and Temporal Distributions of CVOCs at Colorado and New York Vapor Intrusion Sites. *Groundwater Monitoring & Remediation* **2009**, *29*, (1), 70-80.
5. Hosangadi, V.; Shaver, B.; Hartman, B.; Pound, M.; Kram, M. L.; Frescura, C., High-Frequency Continuous Monitoring to Track Vapor Intrusion Resulting From Naturally Occurring Pressure Dynamics. *Remediation Journal* **2017**, *27*, (2), 9-25.
6. McHugh, T.; Beckley, L.; Sullivan, T.; Lutes, C.; Truesdale, R.; Uppencamp, R.; Cosky, B.; Zimmerman, J.; Schumacher, B., Evidence of a sewer vapor transport pathway at the USEPA vapor intrusion research duplex. *The Science of the total environment* **2017**, *598*, 772-779.
7. Pennell, K. G.; Scammell, M. K.; McClean, M. D.; Ames, J.; Weldon, B.; Friguglietti, L.; Suuberg, E. M.; Shen, R.; Indeglia, P. A.; Heiger-Bernays, W. J., Sewer Gas: An Indoor Air Source of PCE to Consider During Vapor Intrusion Investigations. **2013**, *33*, (3), 119-126.
8. Roghani, M.; Jacobs, O. P.; Miller, A.; Willett, E. J.; Jacobs, J. A.; Viteri, C. R.; Shirazi, E.; Pennell, K. G., Occurrence of chlorinated volatile organic compounds (VOCs) in a sanitary sewer system: Implications for assessing vapor intrusion alternative pathways. *Science of The Total Environment* **2018**, *616-617*, 1149-1162.
9. Luo, H., *Field and modeling studies of soil vapor migration into buildings at petroleum hydrocarbon impacted sites* **2009**, Arizona State University Dissertation.
10. Reichman, R.; Shirazi, E.; Colliver, D. G.; Pennell, K. G., US residential building air exchange rates: new perspectives to improve decision making at vapor intrusion sites. *Environmental Science: Processes & Impacts* **2017**, *19*, (2), 87-100.
11. Shirazi, E.; Pennell, K. G., Three-dimensional vapor intrusion modeling approach that combines wind and stack effects on indoor, atmospheric, and subsurface domains. *Environmental Science: Processes & Impacts* **2017**, *19*, (12), 1594-1607.

12. Schuver, H. J.; Lutes, C.; Kurtz, J.; Holton, C.; Truesdale, R. S., Chlorinated vapor intrusion indicators, tracers, and surrogates (ITS): Supplemental measurements for minimizing the number of chemical indoor air samples—Part 1: Vapor intrusion driving forces and related environmental factors. *Remediation Journal* **2018**, *28*, (3), 7-31.
13. USEPA, *OSWER technical guide for assessing and mitigating the vapor intrusion pathway from subsurface vapor sources to indoor air*. US Environmental Protection Agency: 2015.
14. Pennell, K. G.; Scammell, M. K.; McClean, M. D.; Suuberg, E. M.; Moradi, A.; Roghani, M.; Ames, J.; Friguglietti, L.; Indeglia, P. A.; Shen, R.; Yao, Y.; Heiger-Bernays, W. J., Field data and numerical modeling: A multiple lines of evidence approach for assessing vapor intrusion exposure risks. *Science of The Total Environment* **2016**, *556*, 291-301.
15. Abreu, L. D.; Johnson, P. C., Effect of vapor source-building separation and building construction on soil vapor intrusion as studied with a three-dimensional numerical model. *Environ Sci Technol* **2005**, *39*, (12), 4550-61.
16. Pennell, K. G.; Bozkurt, O.; Suuberg, E. M., Development and application of a three-dimensional finite element vapor intrusion model. *J Air Waste Manag Assoc* **2009**, *59*, (4), 447-60.
17. Song, S.; Schnorr, B. A.; Ramacciotti, F. C., Quantifying the Influence of Stack and Wind Effects on Vapor Intrusion. *Human and Ecological Risk Assessment: An International Journal* **2014**, *20*, (5), 1345-1358.
18. Song, S.; Schnorr, B. A.; Ramacciotti, F. C., Accounting for climate variability in vapor intrusion assessments. *Human and Ecological Risk Assessment: An International Journal* **2018**, *24*, (7), 1838-1851.
19. Shirazi, E.; Ojha, S.; Pennell, K. G., Building science approaches for vapor intrusion studies. *Reviews on environmental health* **2019**, *34*, (3), 245-250.
20. Holton, C.; Guo, Y.; Luo, H.; Dahlen, P.; Gorder, K.; Dettenmaier, E.; Johnson, P. C., Long-Term Evaluation of the Controlled Pressure Method for Assessment of the Vapor Intrusion Pathway. *Environmental Science & Technology* **2015**, *49*, (4), 2091-2098.
21. Johnson, P. C.; Holton, C.; Guo, Y.; Dahlen, P.; Luo, H.; Gorder, K.; Dettenmaier, E.; Hinchee, R. E. *Integrated Field Scale, Lab Scale, and Modeling Studies for Improving Our Ability to Assess the Groundwater to Indoor Air Pathway at Chlorinated Solvent Impacted Groundwater Sites*; Arizona State University, Tempe, AZ, United States: 2016.
22. Dols, W. S.; Polidoro, B. J. *CONTAM user guide and program documentation version 3.2*; National Institute of Standards and Technology: Gaithersburg, MD, 2015.
23. US Environmental Protection Agency, Update for Chapter 19-Building Characteristics of the Exposure Factors Handbook. **2018**, *EPA/600/R-18/121F*.

- 1
- 2
- 3
- 4 24. ASHRAE, *2013 ASHRAE handbook : fundamentals*. American Society of Heating,
5 Refrigerating Air-Conditioning, Engineers: Atlanta, GA, 2013.
- 6
- 7 25. ASHRAE, *2001 ASHRAE Handbook: Fundamentals*. American Society of Heating,
8 Refrigerating Air-Conditioning Engineers: 2001.
- 9
- 10 26. Weather Underground.
11 <https://www.wunderground.com/history/monthly/us/ut/ogden/KOGD/date/2010-12>
12 (Date Accessed November 26, 2019)
- 13
- 14 27. Ström, J. G. V.; Guo, Y.; Yao, Y.; Suuberg, E. M., Factors affecting temporal variations in
15 vapor intrusion-induced indoor air contaminant concentrations. *Building and Environment*
16 **2019**, *161*, 106196.
- 17
- 18 28. Y. Guo, C. Holton, H. Luo, P. Dahlen and P. C. Johnson, Influence of Fluctuating Groundwater
19 Table on Volatile Organic Chemical Emission Flux at a Dissolved Chlorinated-Solvent Plume
20 Site, *Groundwater Monitoring & Remediation*, 2019, **39**, 43-52.
- 21
- 22 29. Y. Guo, P. Dahlen and P. Johnson, Temporal variability of chlorinated volatile organic
23 compound vapor concentrations in a residential sewer and land drain system overlying a dilute
24 groundwater plume, *Science of The Total Environment*, 2020, **702**, 134756.
- 25
- 26 30. McAlary, T. A.; Gallinatti, J.; Thrupp, G.; Wertz, W.; Mali, D.; Dawson, H., Fluid Flow Model
27 for Predicting the Intrusion Rate of Subsurface Contaminant Vapors into Buildings.
28 *Environmental Science & Technology* **2018**, *52*, (15), 8438-8445.
- 29
- 30 31. McHugh, T. E.; Beckley, L.; Bailey, D.; Gorder, K.; Dettenmaier, E.; Rivera-Duarte, I.; Brock,
31 S.; MacGregor, I. C., Evaluation of vapor intrusion using controlled building pressure. *Environ*
32 *Sci Technol* **2012**, *46*, (9), 4792-9.
- 33
- 34 32. Lutes, C. C.; Holton, C. W.; Truesdale, R.; Zimmerman, J. H.; Schumacher, B., Key Design
35 Elements of Building Pressure Cycling for Evaluating Vapor Intrusion—A Literature Review.
36 *Groundwater Monitoring & Remediation* **2019**, *39*, (1), 66-72.
- 37
- 38 33. Johnson, P. C.; Ettinger, R. A., Heuristic model for predicting the intrusion rate of contaminant
39 vapors into buildings. *Environmental Science & Technology* **1991**, *25*, (8), 1445-1452.
- 40
- 41 34. USEPA, *User's Guide for Evaluating Subsurface Vapor Intrusion into Buildings*. US
42 Environmental Protection Agency: 2004.
- 43
- 44 35. Weaver, Jim, R. Davis, AND T. Walker. Petroleum Vapor Intrusion Modeling Assessment with
45 PVIScreen. *U.S. Environmental Protection Agency*, Washington, DC, EPA/600/R-16/175,
46 2016.
- 47
- 48
- 49
- 50
- 51
- 52
- 53
- 54
- 55
- 56
- 57
- 58
- 59
- 60

TOC Art

